

The accretion flow in the discless intermediate polar V2400 Ophiuchi

Coel Hellier and A. P. Beardmore

Astrophysics Group, School of Chemistry and Physics, Keele University, Keele, Staffordshire, ST5 5BG

Accepted ???. Received ???

ABSTRACT

RXTE observations confirm that the X-ray lightcurve of V2400 Oph is pulsed at the beat cycle, as expected in a discless intermediate polar. There are no X-ray modulations at the orbital or spin cycles, but optical line profiles vary with all three cycles. We construct a model for line-profile variations in a discless accretor, based on the idea that the accretion stream flips from one magnetic pole to the other, and show that this accounts for the observed behaviour over the spin and beat cycles. The minimal variability over the orbital cycle implies that 1) V2400 Oph is at an inclination of only $\approx 10^\circ$, and 2) much of the accretion flow is not in a coherent stream, but is circling the white dwarf, possibly as a ring of denser, diamagnetic blobs. We discuss the light this sheds on disc formation in intermediate polars.

Key words: accretion, accretion discs – stars: individual: V2400 Oph – novae, cataclysmic variables – binaries: close – X-rays: stars.

1 INTRODUCTION

The magnetic cataclysmic variables can be divided into two classes. In polars (or AM Her stars) the magnetic field of the white dwarf is strong enough to lock its rotation to the binary orbit, and accretion proceeds via a stream which is deflected by the field onto a magnetic pole. In contrast, in intermediate polars (IPs or DQ Her stars) a lower-field white dwarf spins more rapidly than the orbit, and the stream feeds into an accretion disc, which then feeds field lines from its inner edge (see Warner 1995 for a comprehensive review).

The distinction is blurred, however, by the existence of several asynchronous polars, in which the spin periods differ from the orbit by ~ 1 per cent (e.g. Schwöpe et al. 1997). There has also been a long debate on the existence of discless IPs (e.g. Hameury, King & Lasota 1986; King & Lasota 1991; Hellier 1991; Wynn & King 1992). In such systems, the stream would be expected to flip first to the upper pole, then to the lower pole, as the magnetic dipole rotates (e.g. Hellier 1991; Wynn & King 1992). Such pole flipping would occur at the frequency with which the relative geometry changes, namely the beat frequency $\omega - \Omega$, where Ω and ω are the orbital and spin frequencies respectively.

Buckley et al. (1995; 1997) reported the first secure evidence for a discless IP, with the discovery of the *Rosat* source V2400 Oph (RX J1712.6–2414). They found that polarised light from the system varies at 927 s, which is interpreted as the spin period of the magnetic dipole and thus of the white dwarf. The X-rays, though, are pulsed at 1003 s, which is the beat period between the 3.42-h orbital and 927-s spin

cycles; thus V2400 Oph shows the signature of pole-flipping accretion, as expected in a discless IP.

V2400 Oph is a prime opportunity to study the interaction of an accretion stream with a magnetic field in a situation where the flow is continually changing as the dipole rotates. This contrasts with most magnetic cataclysmic variables where the flow is expected to settle (at least temporarily) into a quasi-equilibrium. (In principle the asynchronous polars offer the same opportunity, but it is much harder to obtain good coverage of their ~ 50 -d beat cycles.) In this paper we present new X-ray observations of V2400 Oph, along with optical spectroscopy aimed at tracing the accretion flow as it connects to the field lines.

V2400 Oph is the most polarised IP, leading to a magnetic field estimate of 9–27 MG (Buckley et al. 1995; Våth 1997), the highest for any IP and overlapping with the range for low-field polars. The high field may explain why a disc has not formed in this system, whereas they do in IPs at ~ 1 MG. Buckley et al. (1995) also found that the circular polarisation is always of the same sign, and so concluded that we only ever see one magnetic pole. Given, also, a lack of radial velocity motion at the orbital period, they proposed that V2400 Oph is at a low inclination, and that we only see the pole nearest us (the ‘upper’ pole). From the fact that there were no detectable variations in linear polarisation, Buckley et al. (1995) suggested that this pole was never viewed side on, and so proposed that both the inclination of the binary, and the angle between the spin and magnetic axes of the white dwarf, δ , are low.

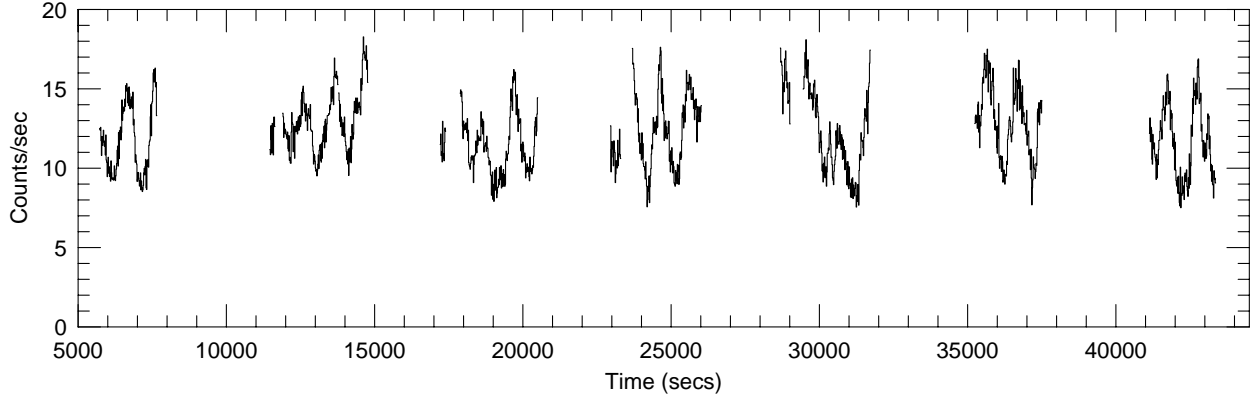


Figure 1. The 2–15- keV X-ray lightcurve of V2400 Oph as recorded by *RXTE*.

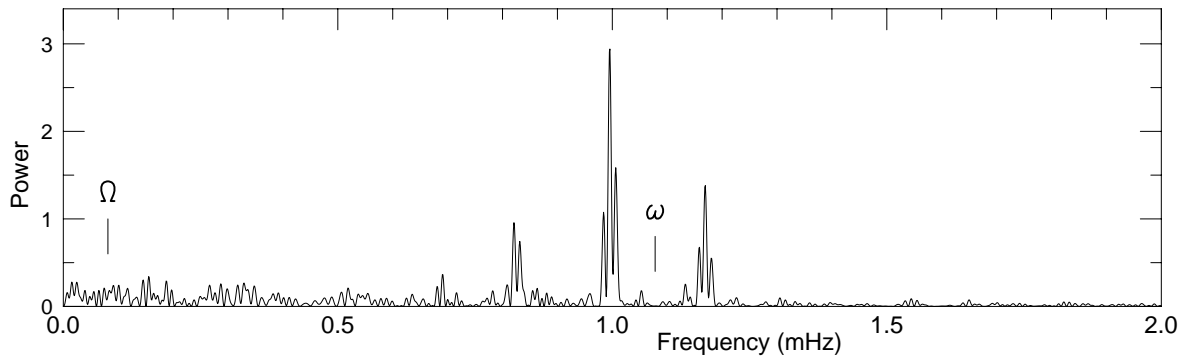


Figure 2. The Fourier transform of the *RXTE* observation, part of which is shown in Fig. 1. The orbital (Ω) and spin (ω) frequencies are marked. The dominant modulation, with an alias structure caused by the spacecraft orbit, is at the beat frequency, $\omega - \Omega$.

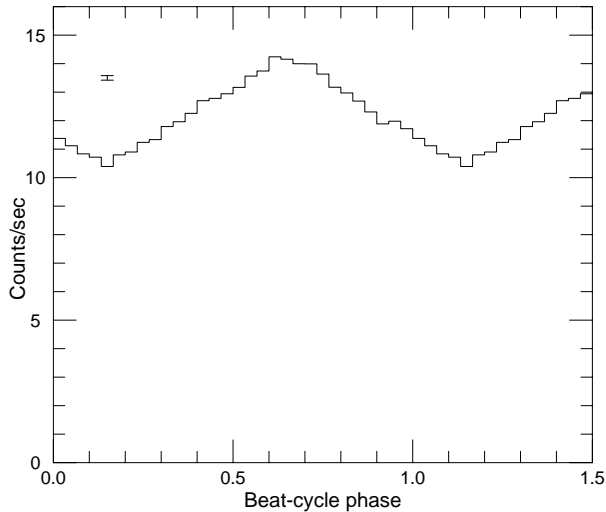


Figure 3. The X-ray lightcurve of V2400 Oph folded on the 1003-s beat period. A typical error is shown.

2 AN *RXTE* OBSERVATION

We report, first, on an *RXTE* X-ray observation obtained over the interval 2000 June 24–25. This resulted in 39 ks of data from the PCA instrument, with either 3 or 4 of the 5 PCU modules in operation at any time. A section of the resulting lightcurve is shown in Fig. 1, while the Fourier

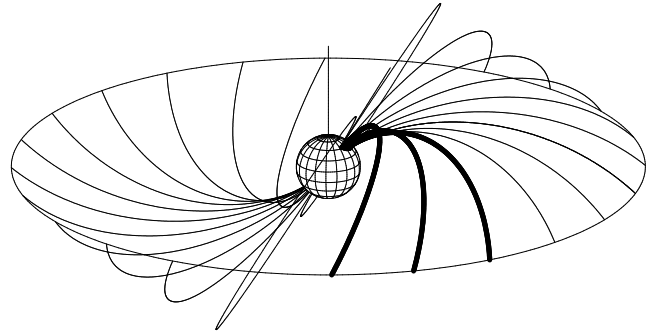


Figure 4. An illustration of the discless accretion geometry in V2400 Oph. In our model (Section 4) the stream attaches to a 20° swathe of field lines (shown in bold). The change in geometry over the beat cycle can be visualised by imagining the feeding point moving round the ring.

transform of the entire observation is shown in Fig. 2. Both lightcurve and transform are dominated by a pulsation at the 1003-s beat period; this has a maximum amplitude of ≈ 50 per cent [(peak–trough)/peak] and a mean amplitude of 25 per cent, as shown by the folded pulse profile in Fig. 3. There is no sign of variations at the orbital period (< 7 per cent) or at the spin period (< 2 per cent). A preliminary look at five other *RXTE* observations, of similar length and spaced at intervals of a few months, finds the same behaviour: a strong beat-cycle pulse but no modulation at the orbital or spin cycles.

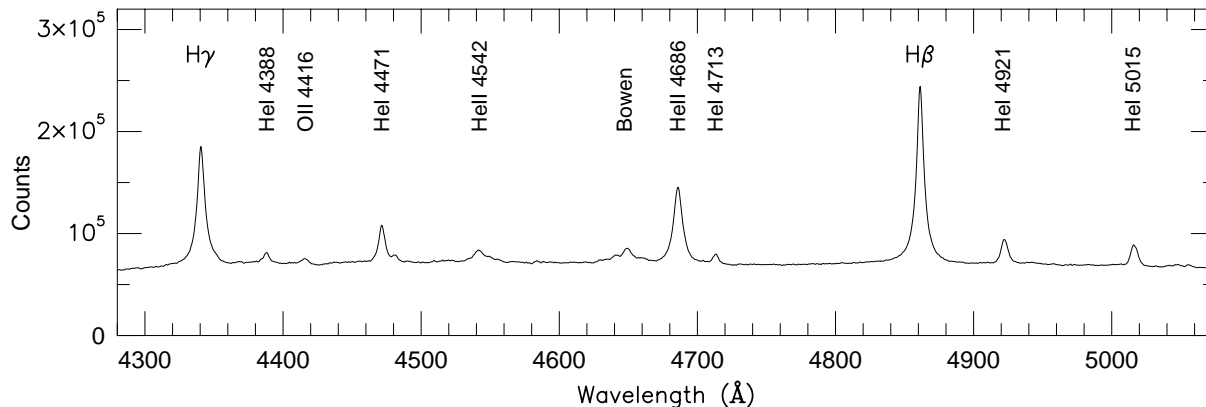


Figure 5. The summed spectrum of V2400 Oph.

The absence of an orbital modulation in the X-ray lightcurve is unexpected in a discless IP. If the stream flows to the magnetosphere, latches onto the nearest field line, and follows it onto the white dwarf (see Fig. 4), then the accretion sites will always be on the hemisphere facing the secondary, and thus their visibility should vary over the orbit, as in an AM Her star. The lack of an orbital modulation can, though, be explained if we concur with the suggestion that V2400 Oph is at so low an inclination that the upper pole is always in view and the lower pole never in view.

The next puzzle arises from the fact that the beat-cycle modulation is not total. If all the accreting material participates in the pole flipping, then, given the low inclination, the flow would flip to the far, hidden hemisphere of the white dwarf for roughly half the beat cycle, leading to 100 per cent modulation. If some of the flow does not flip, but manages to feed both poles continually, then this could explain the non-total modulation. But why, then, does this not result in a spin-cycle pulsation, as seen in all the IPs where a disc ensures continual feeding of both poles? One answer could be to invoke a field aligned exactly with the spin axis, $\delta = 0$, but this would also remove the beat pulse, since nothing would change with beat phase. It also conflicts with the fact that we see spin-cycle variations of the emission lines (see Section 7).

A second answer might be to invoke large, extended accretion footprints, coupled with a large δ so that these sites would be near the white-dwarf equator. In a face-on system, any accretion sites extending across the equator would always be partly in view, and, with both poles partially visible, any pole-flipping modulation would not be total. Arguing against this, however, is the fact that the visibility of the poles would then be exquisitely sensitive to orbital phase, and we do not see any orbital modulation in the X-ray flux. Also, the fact that we see variable circular polarisation but not variable linear polarisation argues that we do not see the poles sideways on (Buckley et al. 1995).

A final possibility could invoke a field geometry that is more complex than a dipole, in which both poles were always on the near, visible hemisphere. However, this is contradicted by the fact that the circular polarisation always has the same sign, arguing that we only see one pole (Buckley et al. 1995). Thus, the absence of an X-ray spin pulse

remains a puzzle, which we defer to Section 8, where we suggest a possible explanation.

3 SPECTROSCOPIC OBSERVATIONS

We observed V2400 Oph with the 3.9-m AAT and the RGO spectrograph plus a TEK CCD. A 1200 lines mm^{-1} grating gave a resolution of 1.4\AA , covering the range $\text{H}\gamma$ to $\text{H}\beta$. Observing for 5.0 h, 4.5 h & 4.5 hr on the three consecutive nights 1996 May 10–12 we obtained 900 integrations of 50 s each, thus covering ≈ 4 orbital cycles and ≈ 50 spin cycle of the star. The summed spectrum, containing He I and He II lines in addition to the Balmer lines, is shown in Fig. 5.

As a first look at the data we computed the equivalent widths and the V/R ratios for the lines in each spectrum (V/R being the ratio of the equivalent widths on either side of the rest wavelength). The Fourier transforms of these quantities for $\text{H}\beta$ and He II $\lambda 4686$ are shown in Fig. 6.

All four Fourier transforms show significant power at the beat ($\omega - \Omega$) frequency, which is always stronger than the power at the spin frequency (ω). A harmonic of the beat frequency, $2(\omega - \Omega)$, is also prominent in the equivalent widths. Other sidebands detected include $\omega - 2\Omega$ in the $\text{H}\beta$ V/R ratios and $2\omega - \Omega$ in the He II $\lambda 4686$ equivalent widths. There is significant power at the orbital frequency in the V/R ratios (a one-day alias being the highest peak) but not in the equivalent widths.

To help us interpret the line profiles of V2400 Oph we have computed simulations of the profiles expected in a discless IP. We first describe this model, and then present a comparison of simulated and observed profiles.

4 MODEL LINE PROFILES

The model we use to simulate the line profiles of V2400 Oph is illustrated in Fig. 4. We assume a dipole field centered at the white-dwarf centre — observations of AM Her stars often indicate the need for a more complex field (e.g. Wickramasinghe & Ferrario 2000) but we know less about the fields in IPs, so adopt the simplest approach. We assume that at some radius, R_{mag} , the stream attaches to the nearest field line and follows this line, taking the gravitationally downhill direction, onto the white dwarf. (Strictly, the field strength,

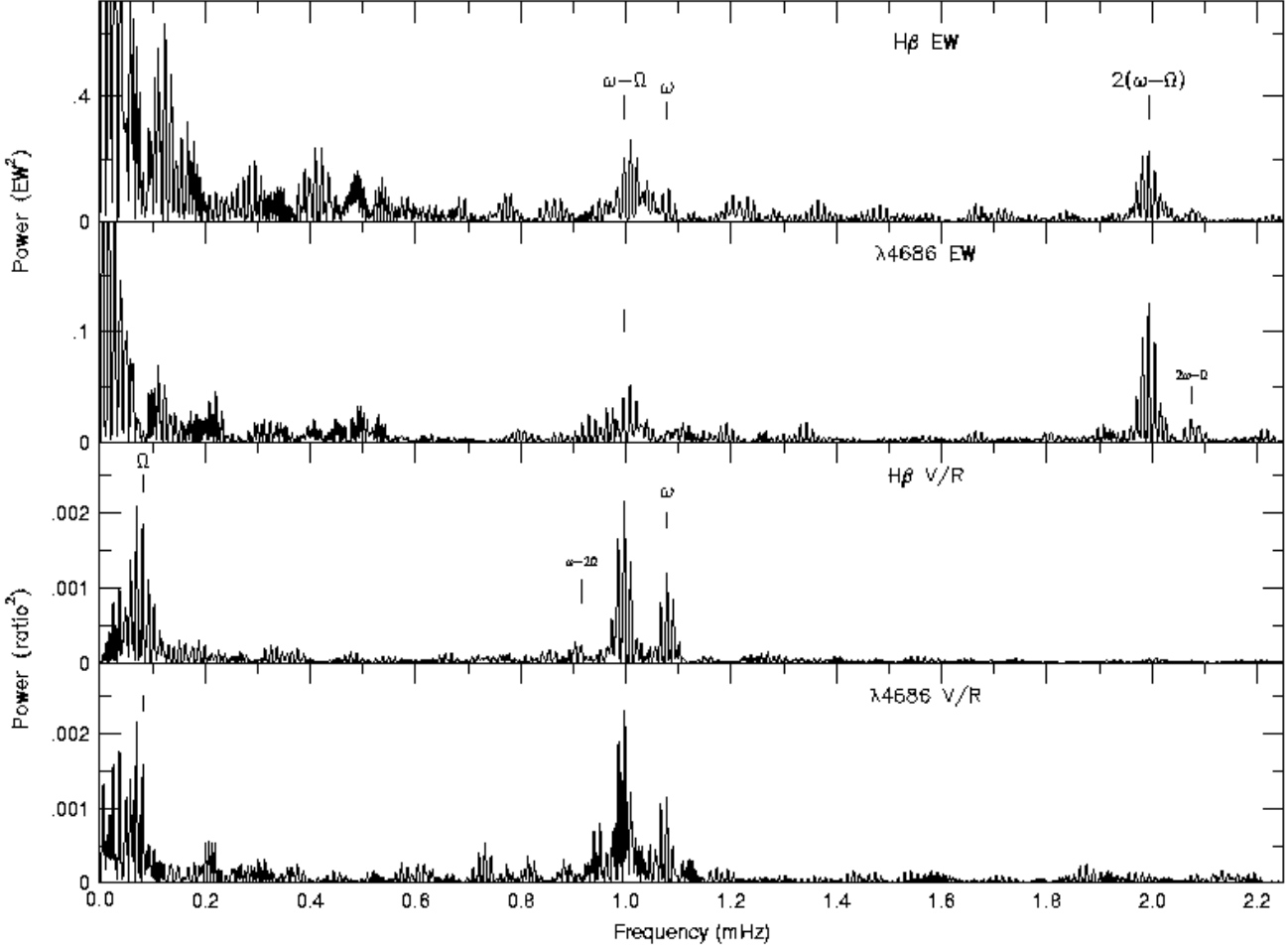


Figure 6. The Fourier transforms of the equivalent widths and V/R ratios of the H β and He II $\lambda 4686$ lines.

and thus R_{mag} , would be a function of the dipole orientation, but how the material feeds onto the field lines, whether it passes through a shock, and how much the rate of feeding depends on dipole orientation are all uncertain, so again we adopt the simplest approach.)

The radius R_{mag} , the angle δ , and the inclination of the binary are all free parameters. We assume, arbitrarily, that the stream feeds a 20° swathe of azimuth. We then calculate the free-fall velocities along the field lines and project them onto the line of sight to produce line profiles. We assume that the emitting regions are optically thick, and so scale the line intensity by projected area. Also, for maximum simplicity, we assume that the field lines are not distorted by their interaction with the flow, and that the material starts infalling with near-zero velocity at R_{mag} , as though it passes through a shock. We also assume that the infall time is short compared to the spin cycle, and thus do not allow for the fact that the stream will have moved on by the time the material accretes. Lastly, we rotate the dipole and stream location to mimic the spin and orbital cycles. We do not include any emission from the stream itself, further out than R_{mag} , which would produce a lower-velocity S-wave on the orbital cycle. Note that the above model is very similar to that developed by Ferrario & Wickramasinghe (1999),

the main difference being that they aimed for model Fourier transforms whereas we aim to compare line profiles.

Fig. 7 shows a sample set of simulated line profiles. We adopted spin and orbital cycles of 927 s and 3.42 h, a white dwarf mass of $0.80 M_\odot$, and a secondary mass of $0.37 M_\odot$. The inclination was 10° , the dipole-offset, δ , was 60° and the radius R_{mag} was $20 R_{\text{wd}}$. The four panels are for emission at different distances from the white dwarf.

A velocity variation at the orbital cycle is obvious in all panels of Fig. 7. Note that this is primarily the infall velocity of the stream, as in an AM Her star, and is not the orbital velocity of the white dwarf, which is much smaller. The spin and beat cycles are seen as the much faster variation in the simulated profiles.

5 LINE PROFILES OVER THE ORBITAL CYCLE

The Fourier transforms (Fig. 6) revealed a variation of the line profiles over the orbital cycle, but when the observed profiles are folded on the orbital cycle it is hardly visible (Fig. 8). To enhance the variation we have subtracted the phase-invariant profile (for each velocity we found the phase bin with the lowest value and subtracted that from

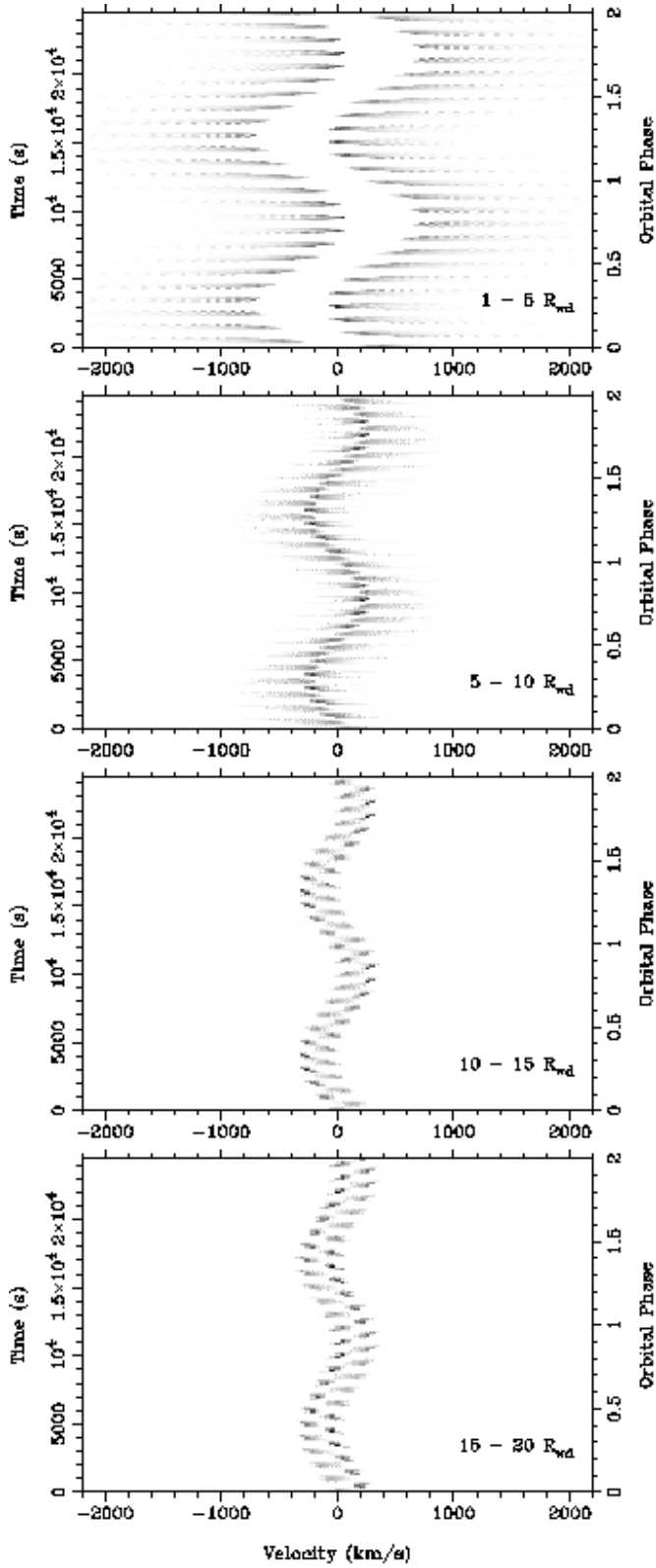


Figure 7. Simulated line profiles in a time sequence covering two orbital cycles. The four panels show profiles for different distances from the white dwarf. Darker colouring signifies stronger emission in all figures.

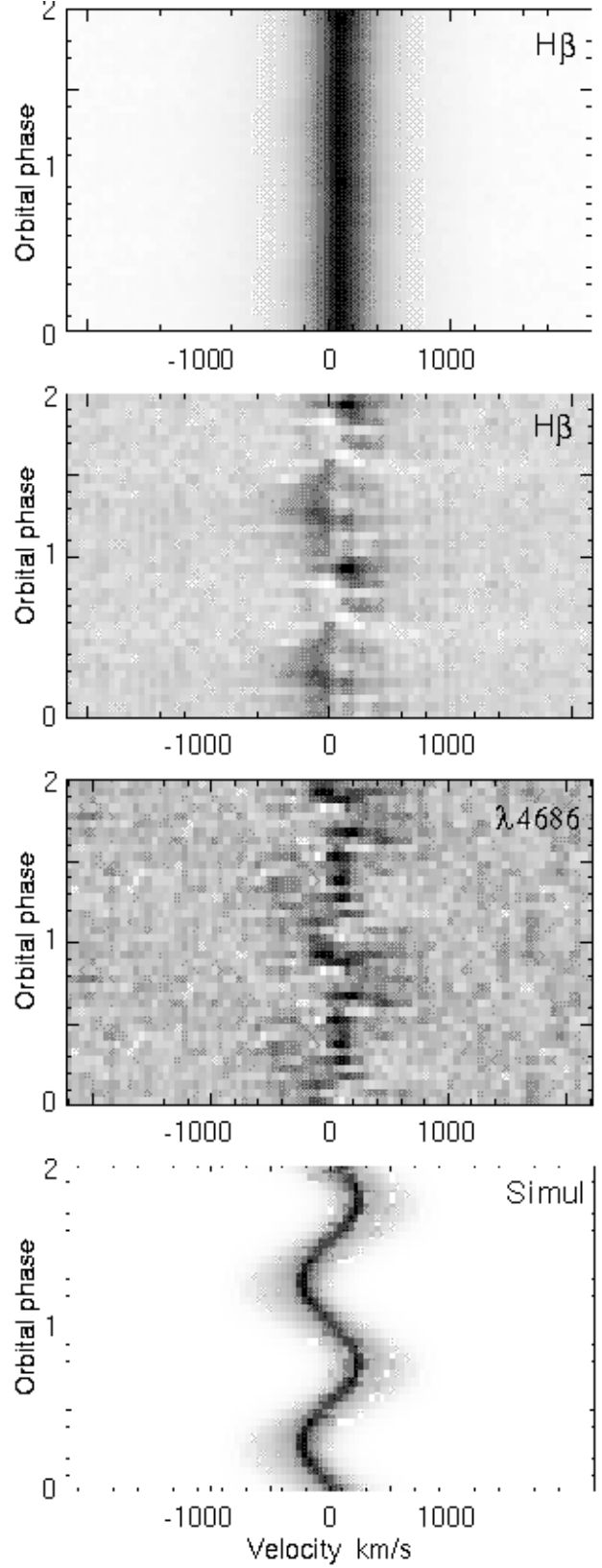


Figure 8. Line profiles folded on the orbital period. The top panel shows the $H\beta$ line; below it are the $H\beta$ and $He II \lambda 4686$ lines after subtraction of the phase-invariant profile. At bottom are the simulated profiles for $5-10 R_{wd}$.

the data). In the portion of the line remaining, only 5 per cent of the original, the slight variation is discernable. Since the orbital modulation is so small, it is clear that V2400 Oph must be at a very low inclination (as already suggested by the X-ray data). But even so, the lack of variation is clearly discrepant with the model, which is calculated for $i = 10^\circ$.

By fitting Gaussians to the phase-resolved $H\beta$ profiles we measure a radial-velocity variation of only 5.8 km s^{-1} , which agrees with Buckley et al. (1995) who report a limit of $< 10 \text{ km s}^{-1}$. If this is the motion of the white dwarf it implies an inclination of only 3° (assuming stellar masses of 0.7 and $0.3 M_\odot$). Even this could be too high, since, as shown by the simulations, we expect the orbital motion to be dwarfed by an infall velocity of anything up to the white-dwarf escape velocity. The observations and simulations can be reconciled only if 1) the system is at an inclination of $< 1^\circ$ (unlikely, since the *a priori* probability is only 1.5×10^{-4}), or 2) much of the emission comes from material that has circularised about the white dwarf and dilutes the emission from the infalling stream. Thus the variations in the emission lines might be tracing only a part (possibly a small one) of the flow.

6 LINE PROFILES OVER THE BEAT CYCLE

Fig. 9 shows the simulated profiles folded on the beat period, again for four distances from the white dwarf. The changes in velocity as the stream changes direction to flow to a different pole are obvious. Note that, at such a low inclination, the dominant component of the velocity is the motion out of the plane following the arch of the field lines. At phase zero the stream is flowing to the upper pole, and the emission $10\text{--}20 R_{\text{wd}}$ out is blueshifted, since it is rising out of the plane towards us; the emission $1\text{--}10 R_{\text{wd}}$ out is falling back to the plane and so is redshifted.

In Fig. 10 we show the observed profiles of $H\beta$ and $\text{He II } \lambda 4686$ folded on the beat cycle. Again, we have first subtracted the phase-invariant profile (leaving only 5 and 10 per cent of the two lines, respectively), since the variation is barely discernable in the raw fold. Accompanying the data are the simulated profiles from $5\text{--}10 R_{\text{wd}}$ out, which give a rough match. The similarity of the $H\beta$ line to the simulation, with both showing changes from red shift to blue shift, suggests that we are seeing the change in velocity as the stream flips from pole to pole. In the observations, however, the flip is less abrupt than in the model, perhaps indicating that the stream feeds field lines over a larger range of azimuth than the 20° adopted in the model. The $\text{He II } \lambda 4686$ line does not match so well, and shows little variation in velocity. Possibly this line comes mostly from near the apex of the arch, where motion out of the plane is minimal.

Our model predicts that the line intensity is modulated at twice the beat frequency (as did the model of Ferrario & Wickramasinghe 1999), and this agrees with the presence of a $2(\omega - \Omega)$ modulation in the equivalent widths (Fig. 6). The weaker modulation seen in the equivalent widths at $\omega - \Omega$ is not predicted by our model, which has symmetric upper and lower poles, but would result from any asymmetry between the poles. Another factor is that X-ray illumination of the stream will vary with beat phase, and this would also modulate the equivalent widths at the beat period.

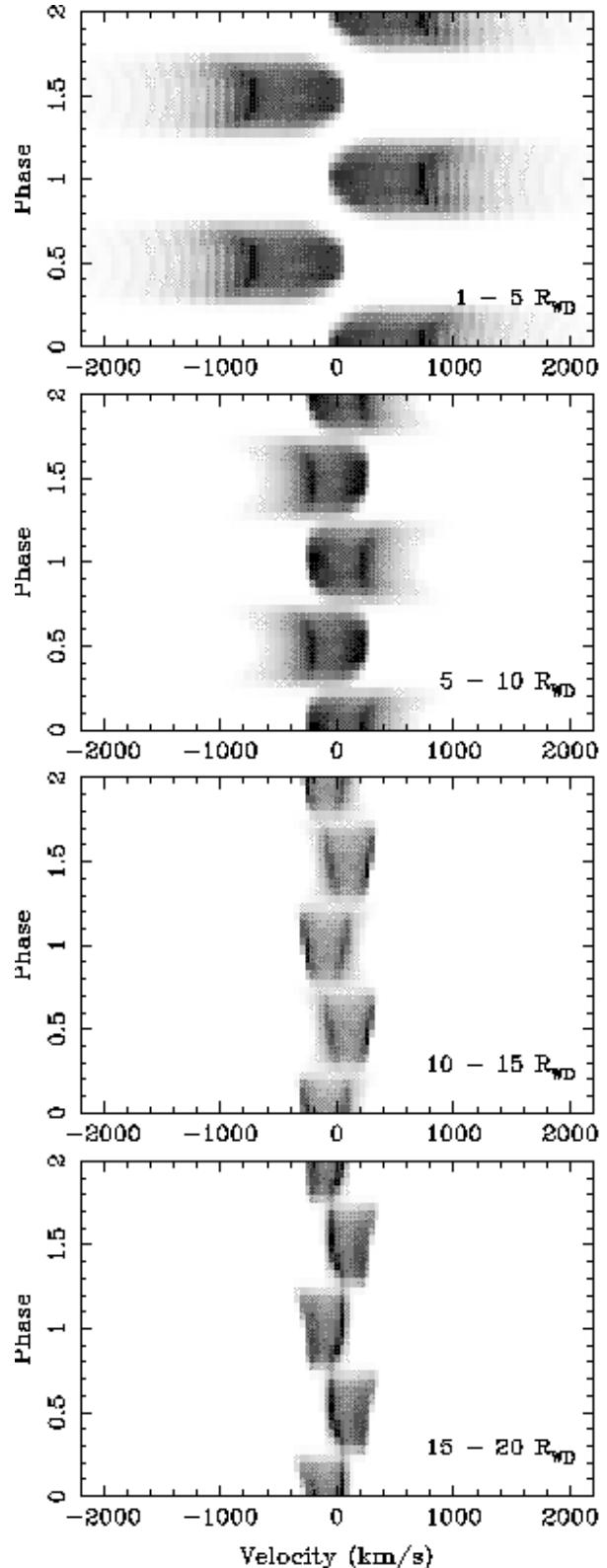


Figure 9. The simulated line profiles folded on the beat period. The four panels correspond to different distances from the white dwarf.

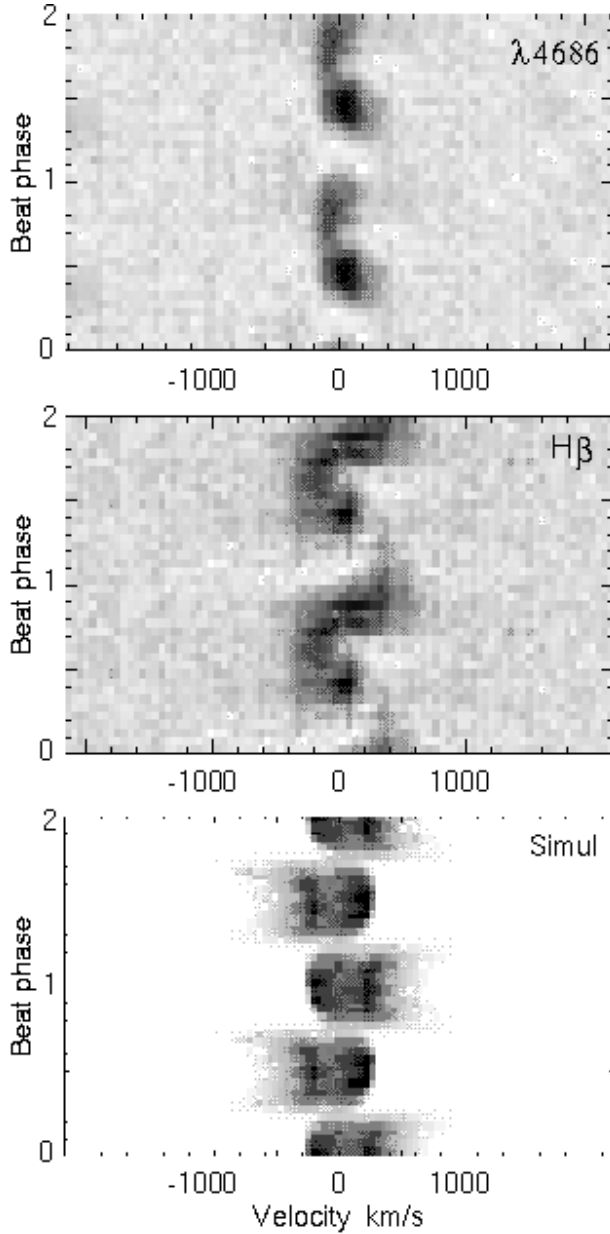


Figure 10. The observed and simulated line profiles folded on the beat period. The data are shown after subtraction of the phase-invariant profile. The relative phasing of data to simulation is arbitrary.

7 LINE PROFILES OVER THE SPIN CYCLE

Fig. 11 shows the simulated profiles folded on the spin cycle. The symmetric shape is the result of the two opposite poles, but note that at any one time only one is accreting. Thus a ‘snapshot’ of the simulation would show an S-wave, snaking from red to blue over the spin cycle; after a pole-flip the inverse S-wave would be seen, and such S-waves accumulate to produce the symmetric pattern when a long sequence is folded.

Again, the dominant velocity is the motion out of the plane, so that the profiles 10–20 R_{wd} out (where material rises out of the plane) tend to show the reverse of the profiles

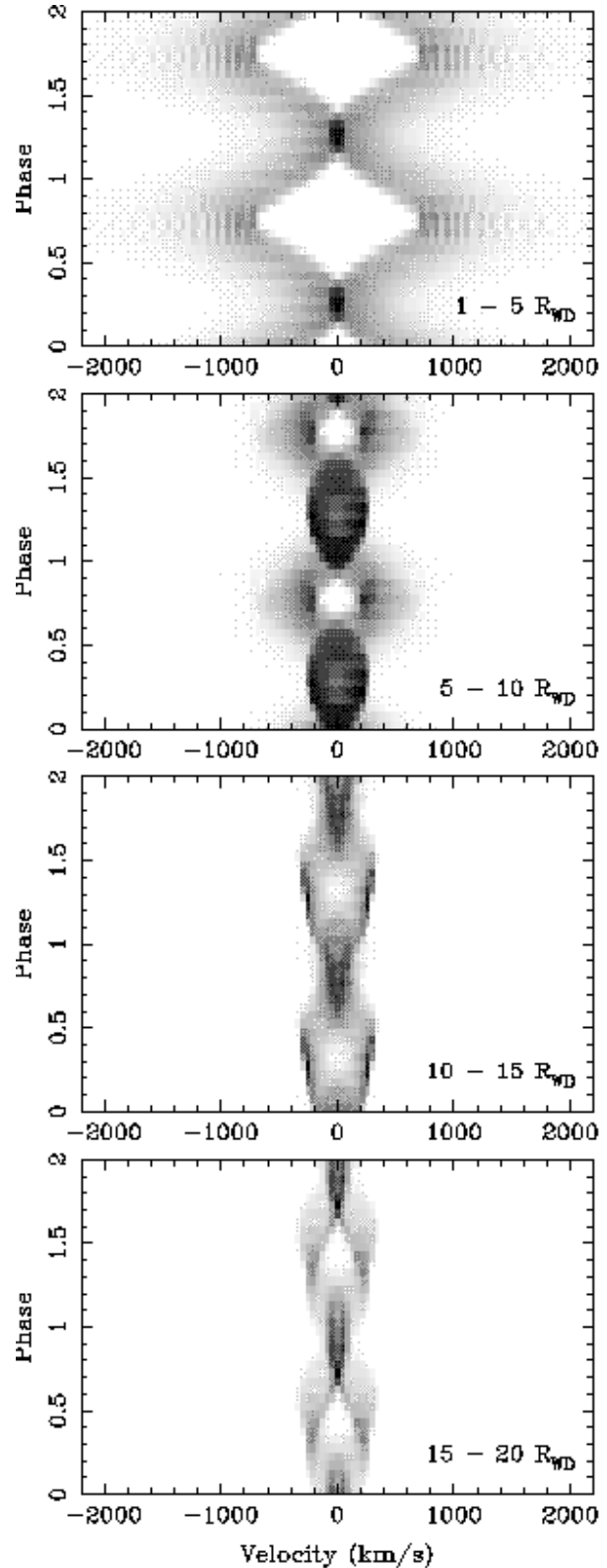


Figure 11. The simulated line profiles folded on the spin period. The four panels correspond to different distances from the white dwarf.

from $1\text{--}10 R_{\text{wd}}$ (where material falls back). If there were no effect of inclination the profiles would repeat exactly twice per spin cycle, but the tilt to an inclination of 10° is enough to break the symmetry.

Fig. 12 shows the spin-folded $\text{H}\beta$ and $\text{He II } \lambda 4686$ profiles, again accompanied with the simulated profiles from $5\text{--}10 R_{\text{wd}}$, which give a good match to the $\text{He II } \lambda 4686$ line. In the simulation the upper pole is at the “3 o’clock” position at phase zero and rotates counterclockwise. At phases $0.2\text{--}0.3$ we are seeing the upper pole furthest from us and the lower pole towards us. The material at $5\text{--}10 R_{\text{wd}}$ is beginning to fall back to the plane. The 10° inclination tilts this motion towards the plane of the sky, reducing the projected velocities, and the profile is thus narrowest. Half a cycle later (upper pole towards us), the inclination tilts the infall motion towards the line-of-sight, and the observed velocities are higher.

The profiles from $\text{H}\beta$ are noisier than those from $\text{He II } \lambda 4686$: after subtraction of the phase-invariant profile only 3 per cent of the original $\text{H}\beta$ line remained. However, the profile can be interpreted as being similar to that of $\text{He II } \lambda 4686$, with the exception that the blue wing seen at phases $0.4\text{--}0.8$ is missing.

7.1 Varying the model parameters

In the previous sections we have compared observed line profiles with models calculated for emission $5\text{--}10 R_{\text{wd}}$ from the white dwarf. We should emphasise that we do not regard the models as fits, since the model contains too many assumptions and adjustable parameters to lead to a unique solution. Instead, we describe here the result of varying the parameters. Since the simulation calculates infall velocities, changing R_{mag} or the white-dwarf mass simply scales the velocities without altering the shape of the model profiles. Similarly, adding an injection velocity at R_{mag} would increase the velocities at all points. Increasing the 20° range of azimuth over which accretion occurs would smear out the profiles, but retain the overall shape.

However, the shape of the spin-resolved profiles is affected by the dipole offset, combined with the inclination. At zero inclination, of course, our view would not change with spin phase and there would be no spin-cycle modulation. This rules out the extreme inclinations of $< 3^\circ$ discussed in Section 5 — only by adopting an inclination of at least 10° do we reproduce the observed spin-resolved profiles, in which the narrow profile at phase ≈ 0.2 changes to a broader, split profile at phase ≈ 0.7 . Even with an inclination of 10° , the profile is only reproduced with $\delta > 30^\circ$: any lower and the change in viewing angle over the spin cycle is insufficient to reproduce the observed profiles. Of course, we can also reproduce the spin-resolved profiles using a higher inclination, but that only increases the problem of the lack of orbital modulation.

8 DISCUSSION

We have shown that the emission lines in V2400 Oph vary on both the spin and the beat cycles, and that the variations are compatible with a model in which the accretion flow

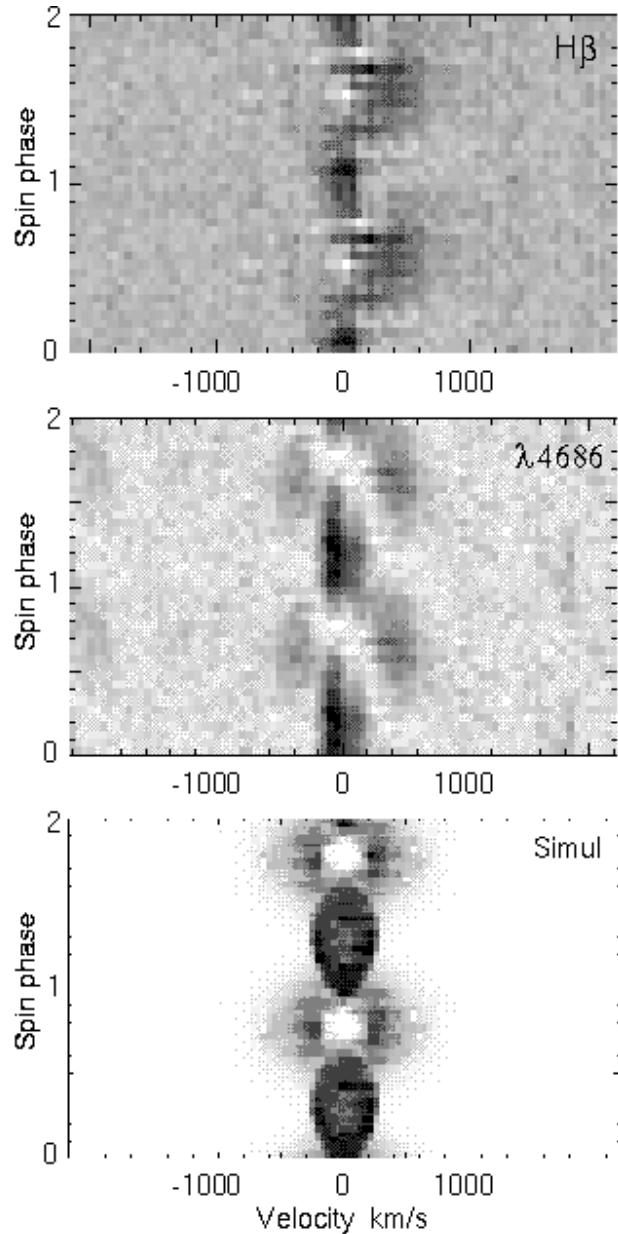


Figure 12. The observed and simulated line profiles folded on the spin period. The data are shown after subtraction of the phase-invariant profile. The relative phasing of data to simulation is arbitrary.

flips from one magnetic pole to the other over the beat cycle — the hallmark of discless accretion in an asynchronous magnetic cataclysmic variable. We have found that a simple model of this behaviour, in which a stream falls to the magnetosphere and then feeds the nearest field line, reproduces the observed line-profile changes over the spin and beat cycles. However, it should be noted that the line-profile variations involve only ≈ 5 per cent of the line emission, and that the bulk of the emission shows no detectable variation.

As a result of this, the variations over the orbital cycle are harder to interpret. We adopt an inclination of 10° , since this is the minimum necessary to reproduce the line-profile

variations over the spin cycle (Section 7). However, if all the emission came from a collimated, infalling stream, this inclination would lead to an orbital modulation of hundreds of km s^{-1} , whereas the observed value is only 5.8 km s^{-1} (Section 5). This implies that the bulk of the emitting material is not in the infalling stream, but is instead symmetric about the white dwarf.

This interpretation is supported by X-ray data, in which the beat-cycle modulation is only 25 per cent deep. Given that the system is at so low an inclination that we only ever see the upper pole, this suggests that only a minority of the accreting material flips from pole to pole, and that there is a continual flow to both poles irrespective of beat-cycle phase.

What is the nature of this flow? One possibility might be a conventional accretion disc. This could feed field lines from its inner edge, forming ‘accretion curtains’ of material in the usual manner for an IP. However, why, then, do we see no X-ray spin pulse? Given that the inclination and dipole offset are sufficient to produce obvious spin-cycle variations in the emission lines, we would expect the aspect of the accretion sites to vary with spin phase, and thus absorption and scattering of X-rays in the accretion curtain would produce a spin pulse (this is best documented in AO Psc; Hellier, Cropper & Mason 1991; Hellier et al. 1996; see also the model of Kim & Beuermann 1995). Another issue is how the stream coexists with the disc, since, having different velocities, they couldn’t both occupy the orbital plane. One plausible answer is that the stream could overflow the disc (see Armitage & Livio 1998 for theoretical simulations of this). This idea has been invoked to explain the IPs showing both spin and beat pulses in the X-ray lightcurves (e.g. Hellier 1991). However, again, a spin-cycle pulsation is nearly always seen, and, taking the example of FO Aqr, the beat-cycle modulation is always weaker or even absent (Norton et al. 1992; Hellier 1993b; Beardmore et al. 1998).

In view of the difficulties in invoking a disc, we turn instead to the idea of magnetically threaded accretion flows, developed by King (1993) and Wynn & King (1995). This model treats the flow as diamagnetic blobs, which are diverted from a ballistic trajectory by the magnetic drag produced by their crossing field lines. The resulting trajectories depend on blob size and density. Simulations by King & Wynn (1999) suggest that it is possible for less-dense matter to be easily threaded and controlled by field lines (which would then act as in our simulations), while denser blobs cross field lines and circulate around the white dwarf. These blobs would lose knowledge of orbital phase, and eventually be destroyed by magnetohydrodynamic instabilities, feeding their material onto the white dwarf’s poles.

Back to the same question, why doesn’t this result in an X-ray spin pulse? We speculate that this process is much less orderly than in a disc-fed accretor. A disc might supply a steady flow over a relatively small disc-magnetosphere transition region, and so feed accretion sites that are small and localised. For example they cover only < 0.002 of the white-dwarf surface in XY Ari (Hellier 1997b). This would lead to steady, well defined accretion curtains, able to absorb or scatter the X-ray flux and so modulate it over the spin cycle. In the diamagnetic-blob model, the accretion sites could be widely strewn and transient; they may not form coherent accretion curtains and so the spin-cycle modulation could be reduced to below the detection threshold.

8.1 Relation to other systems

We have detected variations of the line profiles over the spin frequency in V2400 Oph, whereas hitherto the spin frequency in this star has been seen only in circular polarimetry. This is reassuring, for the following reason. Most IPs show little or no polarised light, and in such systems an X-ray pulse is typically interpreted as the spin period. But if it was actually the beat period, how could we know? The fact that both spin and beat frequencies show up in the line profiles of a discless accretor like V2400 Oph means that we can distinguish between the spin and beat frequencies even without polarimetry. This means that we can unambiguously determine spin frequencies in the class as a whole, since nearly all well-studied IPs show both spin and beat cycles in the emission lines [e.g. Hellier (1997a) and references therein, an exception being TV Col, where neither cycle is convincingly detected in the optical (Hellier 1993a; Augusteijn et al. 1994)].

Secure identification of the spin and beat frequencies strengthens the classification of IPs using the idea that disc-fed accretors show X-ray pulses (predominantly) at the spin cycle while discless accretors show X-ray pulses (predominantly) at the beat cycle. Based on this, we would assign V2400 Oph as the sole secure member of the discless category, and a dozen others to the disc-fed category (e.g. Hellier 1991; 1998). An unclear case is TX Col, in which the spin pulse dominates at some epochs and the beat pulse at others (Norton et al. 1997; Wheatley 1999).

V2400 Oph has a 3.42-h orbit and is the highest-field IP at 9–27 MG. It is likely that this system is on the edge of disc formation since we can account for our observations only if there is a substantial ring-like structure of blobs circling the white dwarf. If the field were a little lower, or the orbit slightly wider (so that the angular momentum of the blobs caused them to orbit further out), the ring of blobs might turn into an accretion disc. Note that PQ Gem, the only IP with a comparable field estimate (9–21 MG; Vāth et al. 1996; Potter et al. 1997) has a wider orbit of 5.19 h (Hellier 1997a). It appears to accrete though a disc, judging by the dominance of the X-ray spin pulse (Mason et al. 1992). It is thus likely that, with these two systems, we are delineating the conditions for disc formation in an IP.

The theoretical requirements for disc formation have long been debated (e.g. Hameury et al. 1986; Lamb & Melia 1988). The issue centers on the three distances R_{\min} (the radius of closest approach to the white dwarf of a ballistic stream from the Lagrangian point), the larger circularisation radius, R_{circ} (where orbiting material has the same angular momentum that it had at the Lagrangian point), and R_{inner} (the radius at which the disc is magnetically disrupted). [We distinguish R_{inner} from the R_{mag} used above since the radius is different for spherical, stream, and disc flows; see Warner (1995) for a fuller discussion and formulae for these radii.]

It is easy to form a disc with $R_{\text{inner}} < R_{\min}$, since the stream could freely orbit outside the magnetosphere, circularise at R_{circ} , and form the disc. It is not possible to form a disc with $R_{\text{inner}} > R_{\text{circ}}$ since the stream has insufficient angular momentum to orbit at these radii. The intermediate case, $R_{\text{circ}} > R_{\text{inner}} > R_{\min}$, is less clear, but is the case applying to most IPs. For example, if we assume that PQ Gem has a red-dwarf mass of $0.5 M_{\odot}$ (appropri-

ate for its 5.19-h orbital period), a white-dwarf mass of $0.7 M_{\odot}$, and that its magnetosphere corotates with the Keplerian orbit at R_{inner} , then, given the 833-s spin period, we have $R_{\text{inner}} \approx 1.1 \times 10^{10}$ cm, which is larger than R_{min} ($\approx 0.6 \times 10^{10}$ cm) and close to R_{circ} ($\approx 1.1 \times 10^{10}$ cm).

V2400 Oph could be showing us the mechanism for disc formation under these circumstances. In this discless system a ring of diamagnetic blobs orbits inside the magnetosphere. In doing so, the blobs cross field lines and lose angular momentum to the field, and so eventually accrete. However, if the field were weaker, as in most IPs, the drag on the diamagnetic blobs would be lower, and their inward spiral would be slower. The blobs might accumulate, screening the field from each other, and so accumulate further in a runaway process leading to the formation of a disc.

9 CONCLUSIONS

- V2400 Oph is at a low inclination, estimated as 10° . We only ever see the upper magnetic pole.
- There is no accretion disc in this system. The stream-fed accretion flips from pole to pole on the beat cycle, and this can be seen directly in the line profiles. However, only ≈ 25 per cent of the accreting material participates in this motion.
- The rest of the material appears to be circling the white dwarf, perhaps in the form of diamagnetic blobs. Such blobs may have been a precursor to disc formation in other intermediate polars.
- The spin-cycle variations of the emission lines are accounted for by a simple model of stream-fed accretion. The best match between model and data is found for distances 5–10 R_{wd} from the white dwarf. The offset between the magnetic and spin axes of the white dwarf must be at least 30° .

REFERENCES

- Armitage P. J., Livio M., 1998, *ApJ*, 493, 898
- Augusteijn T., Heemskerk M. H. M., Zwarthoed G. A. A., van Paradijs J., 1994, *A&AS*, 107, 219
- Beardmore A. P., Mukai K., Norton A. J., Osborne J. P., Hellier C., 1998, *MNRAS*, 297, 337
- Buckley D. A. H., Haberl F., Motch C., Pollard K., Schwarzenberg-Czerny A., Sekiguchi K., 1997, *MNRAS*, 287, 117
- Buckley, D. A. H., Sekiguchi K., Motch C., O'Donoghue D., Chen A., Schwarzenberg-Czerny, A., Pietsch, W., Harrop-Allin M. K., 1995, *MNRAS*, 275, 1028
- Ferrario L., Wickramasinghe D. T., 1999, *MNRAS*, 309, 517
- Hameury J.-M., King A. R., Lasota J.-P., 1986, *MNRAS*, 218, 695
- Hellier C., 1991, *MNRAS*, 251, 693
- Hellier C., 1993a, *MNRAS*, 264, 132
- Hellier C., 1993b, *MNRAS*, 265, L35
- Hellier C., 1997a, *MNRAS*, 288, 817
- Hellier C., 1997b, *MNRAS*, 291, 71
- Hellier C., 1998, *Adv. Space Res.*, 22, 973
- Hellier C., Cropper M., Mason K. O., 1991, *MNRAS*, 248, 233
- Hellier C., Mukai, K., Ishida, M., Fujimoto R., 1996, *MNRAS*, 280, 877
- Kim Y., Beuermann K., 1995 *A&A*, 298, 165
- King A. R., 1993, *MNRAS*, 261, 144
- King A. R., Lasota J.-P., 1991, *ApJ*, 378, 674
- King A. R., Wynn G. A., 1999, *MNRAS*, 310, 203
- Lamb D. Q., Melia F., 1988, in Coyne G. V., ed, *Polarized radiation of circumstellar origin*, Univ. Arizona Press, Tucson, p. 45
- Mason K. O. et al., 1992, *MNRAS*, 258, 749
- Norton A. J., Watson M. G., King A. R., Lehto H. J., McHardy I. M., 1992, *MNRAS*, 254, 705
- Norton A. J., Hellier C., Beardmore A. P., Wheatley P. J., Osborne J. P., Taylor P., 1997, *MNRAS*, 289, 362
- Potter S. B., Cropper M., Mason K. O., Hough J. H., Bailey J. A., 1997, *MNRAS*, 285, 82
- Schwöpe A. D., Buckley D. A. H., O'Donoghue D., Hasinger G., Truemper J., Voges W., 1997, *A&A*, 326, 195
- Väth H., Chanmugham G., Frank J., 1996, *ApJ*, 457, 407
- Väth H., 1997, *A&A*, 317, 476
- Warner B., 1995, *Cataclysmic Variable Stars*, Cambridge University Press, Cambridge
- Wheatley P. J., 1999, in Hellier C., Mukai K., eds, *Annapolis Workshop on Magnetic Cataclysmic Variables*, ASP Conf. Ser., Vol 157, Astron. Soc. Pac., San Francisco, p. 47
- Wickramasinghe D. T., Ferrario L., 2000, *PASP*, 112, 873
- Wynn G. A., King A. R., 1992, *MNRAS*, 255, 83
- Wynn G. A., King A. R., 1995, *MNRAS*, 275, 9